ISSN 0001-4338, Izvestiya, Atmospheric and Oceanic Physics, 2020, Vol. 56, No. 5, pp. 458–469. © Pleiades Publishing, Ltd., 2020.
Russian Text © The Author(s), 2020, published in Izvestiya Rossiiskoi Akademii Nauk, Fizika Atmosfery i Okeana, 2020, Vol. 56, No. 5, pp. 526–539.

Study of the Variability of Spring Breakup Dates and Arctic Stratospheric Polar Vortex Parameters from Simulation and Reanalysis Data

P. N. Vargin[a], *, S. V. Kostrykin[b], **, E. V. Rakushina[c], *, E. M. Volodin[b], ****, and A. I. Pogoreltsev[c], *******

[a]*Central Aerological Observatory, Dolgoprudny, Moscow oblast, 141700 Russia*
[b]*Marchuk Institute of Numerical Mathematics, Russian Academy of Science, Moscow, 119333 Russia*
[c]*Russian State Hydrometeorological University, St. Petersburg, 192007 Russia*
**e-mail: p_vargin@mail.ru*
***e-mail: s_kostr@mail.ru*
****e-mail: zhenya_rakushina@mail.ru*
*****e-mail: volodin@inm.ras.ru*
******e-mail: apogor@rshu.ru*

Received February 6, 2020; revised May 14, 2020; accepted June 3, 2020

Abstract—Five 50-year simulations for the 5th version of the climate model of the Marchuk Institute of Numerical Mathematics, Russian Academy of Science (INM RAS), are used to analyze the interannual variability of Arctic stratospheric polar vortex and dates of spring breakup events (springtime transition) in comparison with reanalysis data. Early spring breakup events are accompanied by stronger wave activity in comparison with late ones. Winter seasons with the maximal air volume in the polar stratosphere and conditions sufficient for the formation of polar stratospheric clouds are characterized by relatively early spring breakup events.

Keywords: climate simulation, spring breakup event, polar stratospheric clouds
DOI: 10.1134/S0001433820050114

1. INTRODUCTION

The winter stratospheric circulation in the Arctic is characterized by strong interannual variability, which is mainly determined by the wave activity propagating from the troposphere. However, the stratosphere not only responds to wave-activity propagation, but also affects it. The study of the variability of the Arctic stratospheric circulation is urgent because of its effect on the state of the stratospheric ozone; the upper atmosphere [1]; and the troposphere, which is important for improving seasonal weather forecasts [2–5].

Despite the recent decrease in the content of ozone-depleting compounds in the atmosphere, significant ozone-layer negative anomalies can occur in the Arctic up to the middle of the 21st century, comparable to the record ozone loss in spring 2011 [6, 7], which can induce high UV radiation levels over the next several months [8]. A sudden stratospheric warming (SSW) event at the end of January 2016 prevented ozone depletion, which was more severe than in 2011 [9]. Significant ozone depletion was observed in the Arctic stratosphere in spring 2020. Stratospheric ozone anomalies in the Arctic in 1980–2000, which took place in winter seasons without SSWs, could affect the temperature and wind in the troposphere and precipitation regime, and the effects could be the strongest in the North Atlantic and Eurasia in April–May [10]. In the Antarctic stratosphere, significant ozone depletion is observed every spring with rare exceptions, but the strongest were in 2011, 2015, and 2018 [11].

A spring breakup event (springtime transition), or a final SSW, is an annual change in the direction of the zonal circulation usually observed in early April. One distinctive feature of a spring breakup event is an irreversible change in the zonal wind direction until the onset of the next winter season, in contrast to SSWs, after which the western (from west to east) zonal wind often recovers in 1–2 weeks [12]. Spring breakup events are observed in both hemispheres, their dates and features of development are determined by the radiation effect (enhancement of heating of the stratosphere due to an increase in solar azimuth), the wave activity propagating from the troposphere, and the state of the stratosphere [13, 14]. Spring breakup dates and their interannual variability is an important climate factor in extratropical latitudes of the Northern Hemisphere, which affects the hydrological cycle, vegetation, and ecosystem productivities [15].

Differences in tropospheric circulation (in the geopotential, zonal wind, and storm track activity) were revealed over the Euro-Atlantic region in April for the cases of early and late spring breakup events [16]. In addition to their dates, it was suggested to divide the events to those which originate in the middle stratosphere near 10 hPa (~30 km) and in the upper stratosphere near 1 hPa (~50 km) [17]. Spring breakup events of type 1 are accompanied by a stronger negative phase of North Atlantic Oscillation (NAO) than events of type 2. Based on the UKMO reanalysis data, early spring breakup events have been shown to be accompanied by an increase in the amplitude of a stationary planetary wave with a zonal number equal to 1 (SPW1) in March; the wave activity is weaker in the case of late spring breakup events, and they are is due to seasonal heating of the middle atmosphere [18]. A trend toward a later occurrence (delay) of late breakup events is revealed, which can be associated with a decrease in the amplitude of SPW1 in March [18].

The analysis of long-term ensemble calculations within the WACCM chemical–climatic model have shown that changes in the stratospheric polar vortex due to the major SSWs in the previous winter lead to a later occurrence of spring breakup events, which start near 10 hPa. The interannual variability of the breakup events can be affected by quasi-biennial ocsillation (QBO) of the zonal wind in the equatorial stratosphere and by the ocean surface temperature [19]. Early breakup events in winter seasons without major SSWs often lead to the formation of "frozen" anticyclones in the Arctic stratosphere [20], which contain air masses from low latitudes, for example, like in April–May 2011 [21].

Data from 11 predictive systems from the S2S seasonal prediction project have allowed differences in the predictability of early and late spring breakup events to be revealed: the former are less predictable than the latter [22]. The type of breakup dates (early or late) for the average values over the ensemble of the predictive systems analyzed is forecasted for 4 weeks.

A spring breakup event determines the period of destruction of the stratospheric polar vortex, inside which the temperature in winter can drop to extremely low values winter, sufficient for the formation of type I polar stratospheric clouds (PSC) (at $T < -78°C$), which mainly consist of nitric acid trihydrate ($HNO_3–3H_2O$) solid particles, and type II PSC (at $T < -85°C$), which consist of ice crystals. Type II PSCs are predominantly observed in the Antarctic stratosphere. The main air volume inside a polar vortex with temperatures sufficient (or with a potential) for the PSC formation (hereinafter, the PSC volume) is formed in the lower stratosphere at altitudes of 15–21 km. This parameter is often used to assess the degree of ozone depletion: its value averaged over a winter season is linearly connected with the total magnitude of the chemical ozone depletion [23, 24].

Heterogeneous activation of the chlorine and bromine components, which are in the ozone-neutral state and come from the troposphere from anthropogenic sources, occurs on the PSC surface during the polar night [23]. When sunlight penetrates into the polar stratosphere, these chlorine and bromine components (for example, Cl_2) release chlorine and bromine atoms, which quickly react with ozone and destroy it with formation of also rapidly destroying compounds (for example, Cl_2O_2), which again release chlorine and bromine atoms. It is these catalytic reactions with the participation of activated chlorine and bromine that are the most destructive for the ozone layer.

Model calculations have shown the defining contribution of wave activity on the conditions for PSC formation inside the Arctic stratospheric polar vortex; in Antarctica, wave activity affects the degree of stability of the stratospheric polar vortex and the strength of the ozone-layer anomalies [25].

Spring breakup events mainly occur due to stronger heating of the stratosphere because of an increase in solar irradiation. However, dynamic processes, such as the nonlinear interaction of the mean flow with planetary waves, can affect the character and time (date) of their onset. This is reflected in the interannual variability of the spring breakup dates, which can take place from early March to late May [18].

The aim of this work is to estimate the reproduction of the spring breakup dates in the Arctic in calculations within the INM RAS climate model and their variability, as well as the air volume inside the polar vortex with temperatures sufficient for PSC formation.

2. ANALYSIS TECHNIQUES AND DATA USED

2.1. INM RAS Climate Model

Five 50-year (1965–2014) ensemble model calculations in the INM RAS climate model version 5 [26] are used. The calculations were carried out within the CMIP6 international project for comparing climate models. The above 50-year calculations complete the model experiment on the historical climate from 1850 to 2014.

First, a preindustrial 1200-year experiment was carried out within the model, with all forcings and emissions fixed to 1850 year. The model states corresponding to January 1 of different years (prognostic parameters for the atmosphere: temperature, specific humidity, wind speed, and surface temperature; prognostic parameters for the soil, ocean, and aerosols) were taken from that experiment and used as source data for the five historical experiments analyzed in our work. Those states were considered corresponding to the start of each experiment, i.e., January 1, 1850. The idea of the analysis of the ensemble of historical experiments is the following: if time variations in a parameter are similar in all the experiments, then they are due to a change in the forcings on the climate system. If the variations are different,

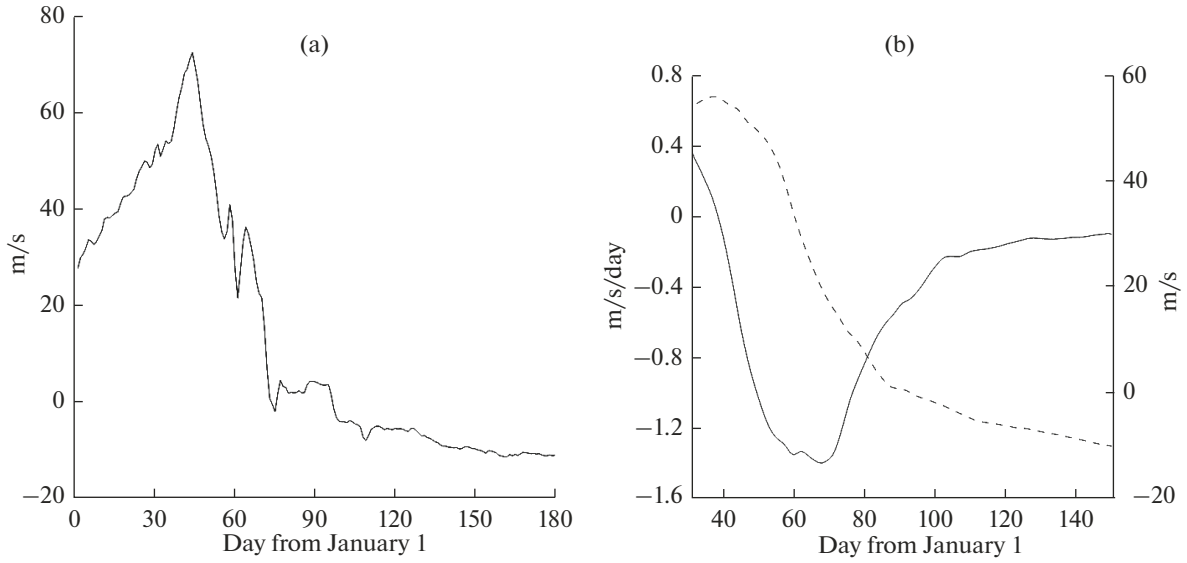

Fig. 1. (a) Variation in the zonal mean wind (m/s); (b) smoothed variation in the zonal mean wind (dashed curve, right scale) and smoothed rate of the variation (m/s day) (solid curve, left scale) at 10 hPa and 62.5 N from February 1 to May 31, 1987, according to the ERA-Interim reanalysis data.

then these differences are due to the natural variability in the climate system.

The spatial resolution of the model is 2° longitude × 1.5° latitude × 73 vertical levels up to 0.2 hPa (~60 km) in the atmosphere and 0.5° × 0.25° × 40 vertical levels in the ocean. Version 5 of the model differs from the previous ones in higher vertical resolution in the upper stratosphere and lower mesosphere, better parameterization of large-scale condensation and cloudiness, and the addition of the aerosol block [27]. As a result of the improvement, the INM RAS model reproduces the QBO of zonal wind oscillations in the equatorial stratosphere and a close-to-actual SSW frequency. The results of the analysis of dynamic processes in the Arctic stratosphere and the dynamic stratosphere–tropospheric coupling in the INM RAS climate model are presented in [28–30].

The forcings on the climate system were specified in the model calculations following CMIP6 Project recommendations: those of CO_2, CH_4, and N_2O, in the form of annual average concentrations averaged over the air column; those of volcanic aerosol in the form of monthly average concentrations versus latitude and altitude; those of ozone in the form of monthly average concentrations versus longitude, latitude, and altitude taking into account the ozone layer depletion since the early 1980s; and those of anthropogenic emissions of SO_2 and black and organic carbon in the form of monthly average values versus longitude and latitude.

2.2 Analysis of Polar Stratospheric Clouds

The PSC volume was estimated from the simulation data based on the preliminary calculation of Arctic stratospheric polar-vortex parameters according to [31]. Using 3D daily data on the air temperature, wind speed, and geopotential, the potential vorticity (PV) on isobaric surfaces was calculated. Then, the PV and temperature values were interpolated to isentropic levels, where the maximum of the PV derivative with respect to the equivalent latitude was calculated, and the corresponding PV value was taken as the vortex boundary. Further, those values were averaged over December–March and used to determine the climatological boundary of the polar vortex. The resulting parameters were used for estimating the daily area of the polar vortex. The critical temperature values from [31] were used to assess the area with the potential for the formation of type I PSCs. At each isentropic level, a grid cell was related to the PSC region if it was both inside the polar vortex and its temperature is below the critical temperature. The PSC and the polar-vortex volumes were calculated for the altitude range from 390 to 590 K (~120–30 hPa) from the known area at each level and the thickness of the isentropic layers via summing the areas at different heights with corresponding weight factors.

2.3. Determination of Spring Breakup Dates

There are different techniques for determining the date of a spring breakup event [22], for example, by the time when the region within a given isoline of the vorticity, which characterizes the strength of the stratospheric polar vortex, drops below a certain value [32], or when the zonal wind speed drops below zero or another critical value selected [13, 32]. Such estimations are ambiguous, since the zonal wind speed can fluctuate around a value close to zero for quite a long

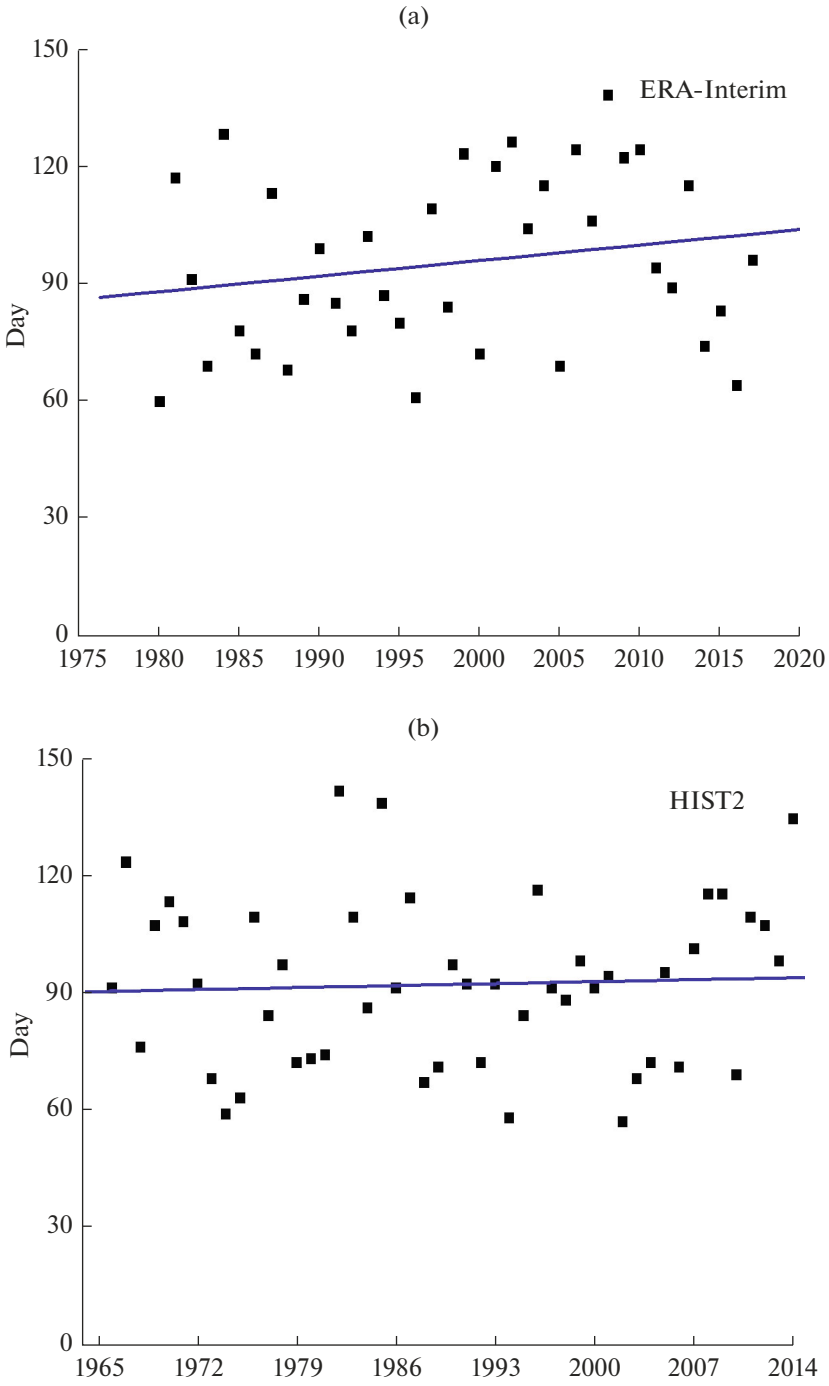

Fig. 2. Spring breakup dates according to (a) ERA-Interim data from 1980 to 2017 and (b) HIST2 model calculation from 1965 to 2014.

time, which complicates the determination of the spring breakup period [18]. This can be seen on the example of fluctuations of the zonal mean wind at 10 hPa (~32 km) and 62.5 N from January to late June 1987, according to ERA-Interim data (Fig. 1a). The choice of a specific vorticity isoline and other critical values are quite subjective [13]; therefore, the spring breakup-event criteria are also subjective.

We used the technique where the breakup event date is defined as the day with the maximal absolute rate of decrease in the zonal wind at 10 hPa and 62.5 N near the maximum of the zonal jet stream [18]. Since the rate of change in the zonal wind strongly fluctuates, its time gradients were calculated from the values smoothed over 31 days in order to determine the absolute minimum of the rate. The spring breakup event in

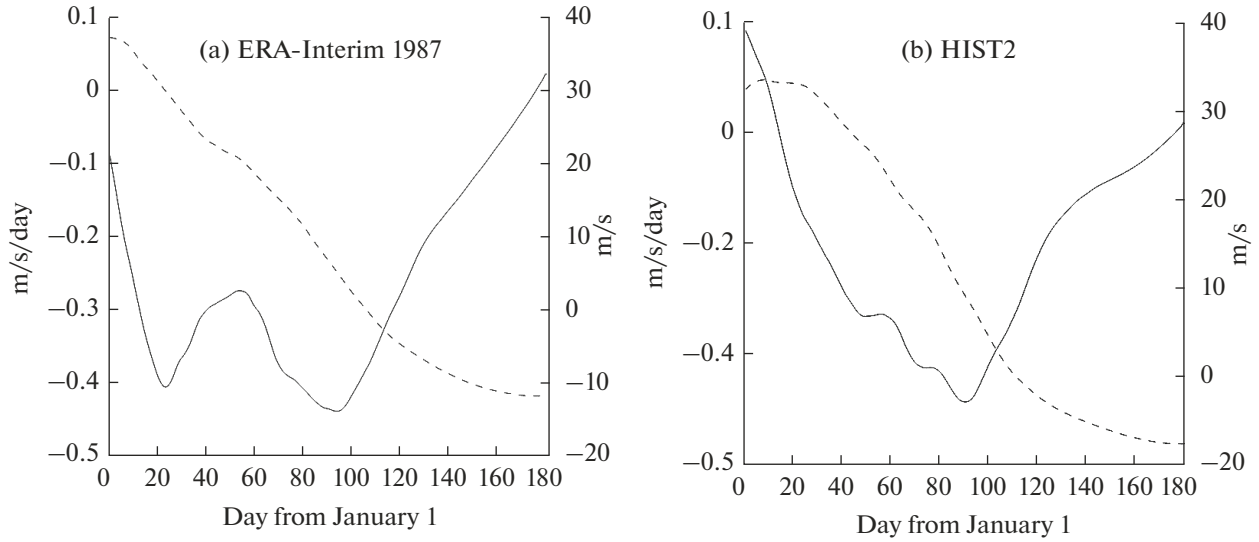

Fig. 3. Variation in the zonal mean wind (m/s) (dashed curve) and smoothed rate of the variation (m/s day) (solid curve) at 10 hPa and 62.5 N from January 1 to June 30 according to (a) ERA-Interim data when averaging over 1980–2017 and (b) HIST2 model calculation when averaging over 49 winter seasons.

1987 falls on the 68th day, i.e., March 10 (Fig. 1b). The dotted curve shows the same zonal wind as in Fig. 1a, but smoothed. The solid curve shows the rate of change in the zonal wind (with the same smoothing); its absolute minimum falls on the 68th day. That technique was used for determining the spring breakup dates for each year from the ERA-Interim reanalysis data for 1980–2017 and five INM RAS model calculations.

3. RESULTS

3.1. Spring Breakup Events

The model spring breakup date varies within a 2-month range, from March to April, which is consistent with the estimates from the reanalysis data. Figure 2 shows variations in the spring breakup dates at 10 hPa and 62 N found from the ERA-Interim reanalysis data from 1980 to 2017 and from the HIST2 model experiment over 49 years. The days are counted from January 1; the 59th day is March 1 and the 151st day is May 31. There is a noticeable (insignificant) trend in the shift of the breakup dates toward later ones according to the reanalysis data. The variability of the spring breakup dates is consistent with the results obtained from the NCEP reanalysis data [18], where a significant positive trend toward later spring breakup dates was revealed over a period of 41 years. Only the HIST2 experiment shows comparable variability of the breakup dates. Other experiments are characterized by a weak negative trend, but the distribution is more neutral in general.

The climatological date of the spring breakup event was calculated from data of ERA-Interim reanalysis for 1980–2017 and for each model experiment HIST1–5. It was found to be April 4, or the 94th day (Fig. 3). The climate dates of spring breakup events found in the model experiments are given in Table 1 (column A). They are close to the date found from the reanalysis data; the maximal difference is 8 days.

Table 1. Climate dates of spring breakup events in the HIST1–5 model calculations and the reanalysis data (column I), correlation coefficient of the spring breakup dates and the SPW1 amplitude at 10 hPa and 62 N in March (column II), and coefficient of correlation between the spring breakup dates and the total PSC volume in winter (column III). Statistically significant (95% by the Student's test) correlation coefficients are shown in bold

	I	II	III
HIST1	April 1 (the 91st day)	**–0.29**	0.03
HIST2	April 4 (the 94th day)	**–0.53**	–0.07
HIST3	March 27 (the 86th day)	**–0.46**	**–0.28**
HIST4	April 1 (the 91st day)	–0.26	–0.2
HIST5	March 28 (the 87th day)	–0.17	–0.17
ERA-Interim	April 4 (the 94th day)	**–0.62**	**–0.34**

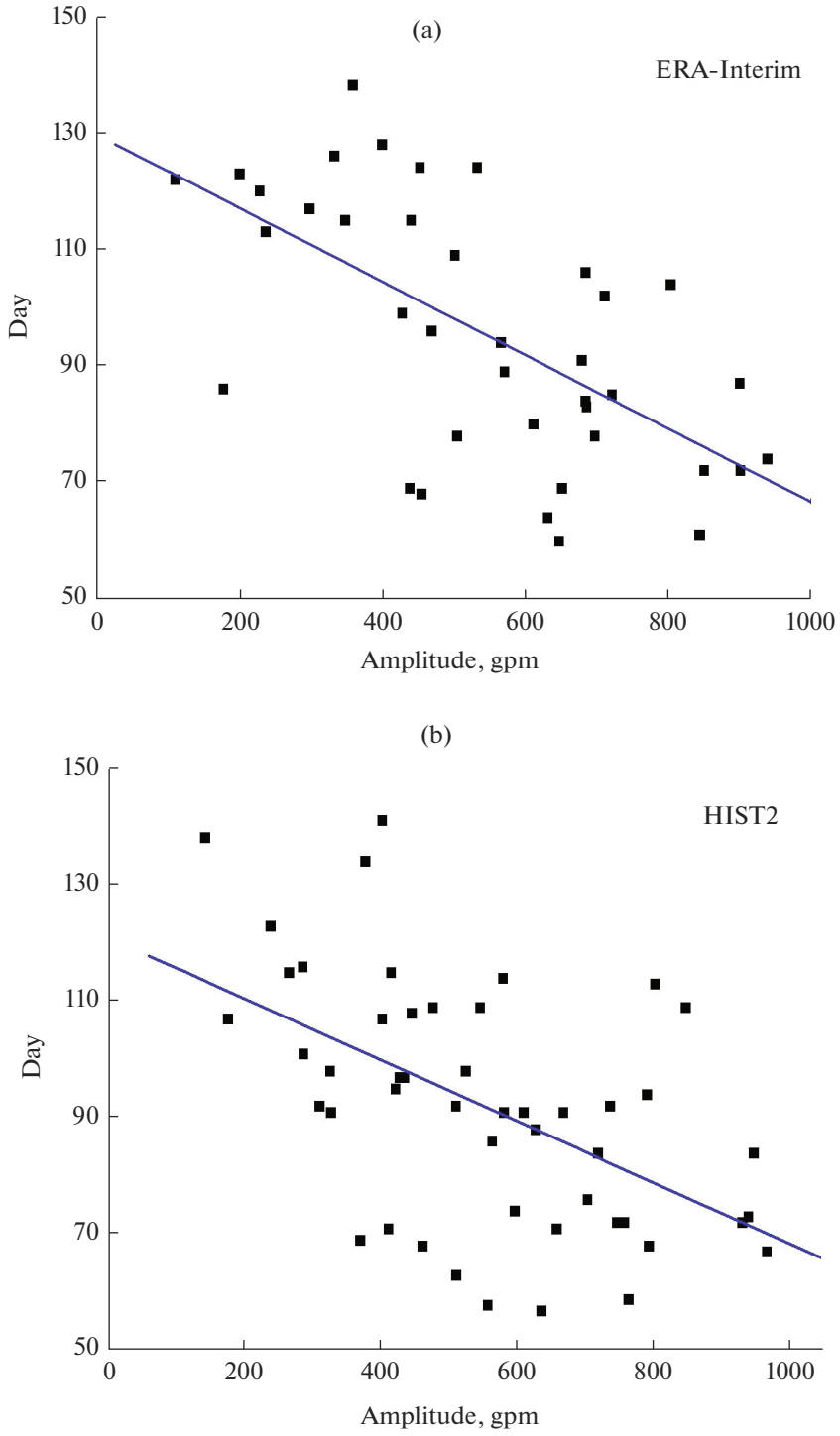

Fig. 4. Scatter diagram of the SPW1 amplitude in March at a pressure level of 10 hPa and spring breakup dates according to (a) ERA-Interim reanalysis data and (b) HIST2 model calculation results.

As was already noted, planetary waves can significantly affect the spring breakup date. The analysis of planetary waves shows early breakup events to be accompanied by an increase in the SPW1 amplitude, while the wave activity is weaker during late breakup events, and they are caused by seasonal heating of the middle atmosphere [18]. Moreover, the SPW1 amplitude decreased in the lower stratosphere and increased in the upper stratosphere [33, 34] in recent years.

Figure 4a shows the scatter diagram of the SPW1 amplitude in March at 10 hPa and the spring breakup dates according to reanalysis data. A similar curve for

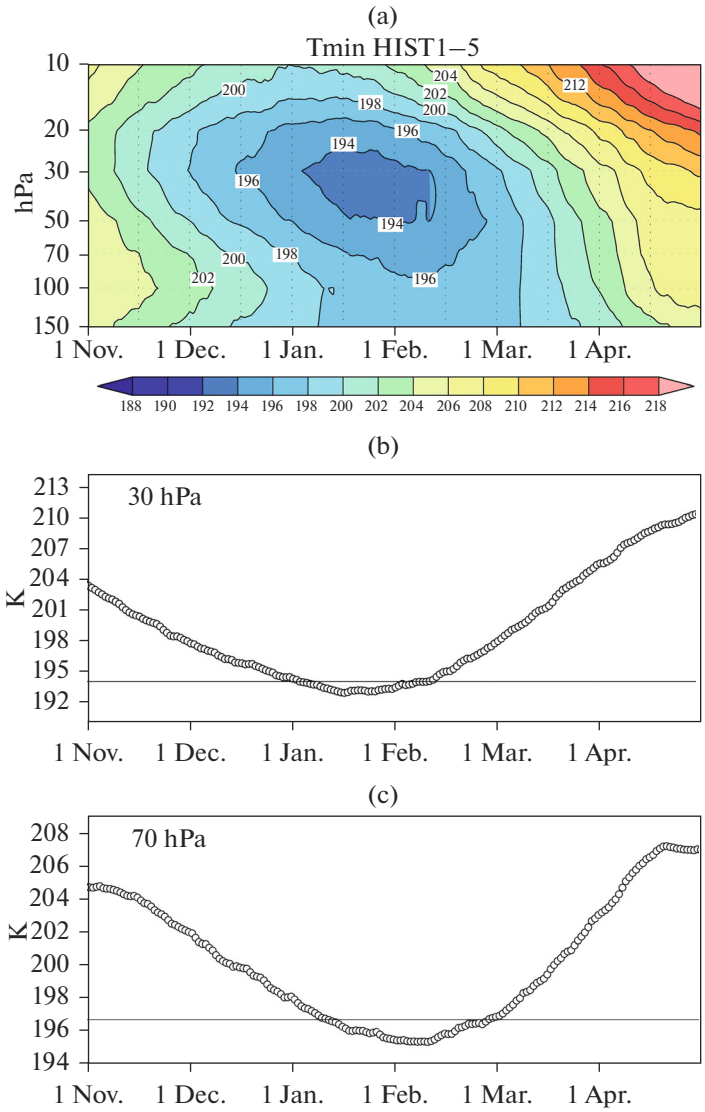

Fig. 5. Seasonal variations in climate values (1979–2014) of Arctic stratospheric polar vortex parameters averaged over HIST1–5 experiments: (a) minimal temperature in the Arctic stratosphere at pressure levels from 150 to 10 hPa and (b) separately for a level of 30 and (c) 70 hPa; (d) regions $T < T_{nat}$ in the Northern Hemisphere (% of the hemisphere area) for the pressure range from 150 to 10 hPa and (e) separately for 30 and (f) 70 hPa.

the HIST2 calculation, with the highest negative correlation among all calculations (Table 1), is plotted in Fig. 4b for comparison. A linear correlation is observed between the SPW1 amplitude and the spring breakup dates. The linear correlation coefficient is –0.62 for the reanalysis data and –0.53 for the HIST2 calculation. Both coefficients are statistically significant, with a significance level of 95% by Student's test. If planetary waves are stronger in March, spring breakup events occur earlier. The pattern is similar for other calculations, although the correlation coefficients for the HIST4-5 calculations are minimal and statistically insignificant.

Thus, dynamic processes affect the stratospheric circulation during spring breakup events. On the other hand, the effect of SPW1 on the spring breakup date may be indirect and connected with other processes. For example, the breakup date can depend on the QBO phase (east/west) or the Madden–Julian oscillation, which affects the zonal flow and can impede the planetary wave propagation by shifting the spring breakup event to a later date [35].

3.2. Estimation of Parameters of Polar Stratospheric Clouds

The seasonal variations in the minimal climate average temperature of the Arctic stratosphere are shown in Figs. 5a–5c. A comparison with similar figures for the reanalysis ensemble mean (REM) [31]

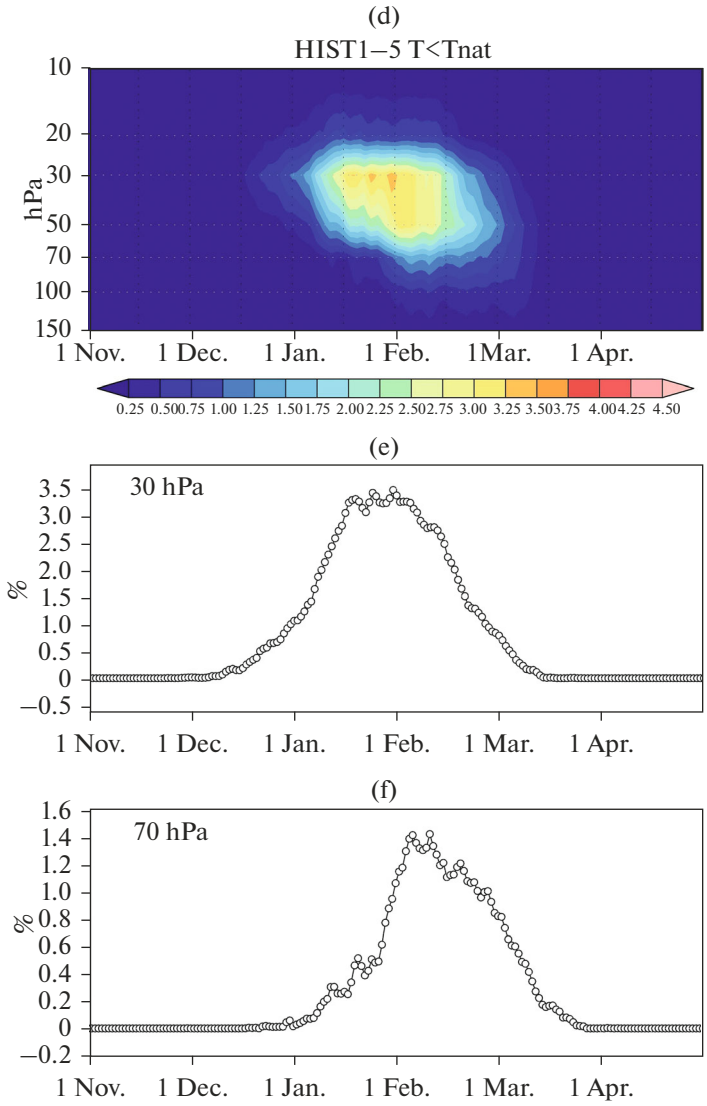

Fig. 5. (Contd.)

allows one to conclude that the REM temperature minimum occurs earlier, from mid-to-early December, and at higher altitudes, at 20–30 hPa, than in the INM RAS model data (from early January at altitudes of 30–40 hPa). Extremely low temperatures end at about the same time.

An analysis of the intraseasonal variability in PSC on the basis of the model data shows their maximal area (the region with conditions sufficient for the PSC formation) to approximately correspond to that calculated from the REM data (Figs. 5d–5f). However, as in the case of extreme temperatures, PSC in the INM RAS model data appear half a month to a month later and disappear at about the same time as in the REM data (early-to-mid March).

The time dependences of the polar stratospheric vortex parameters in the HIST1-5 model experiments calculated by the techniques [31, 36] are shown in Fig. 6, including the December–March averaged relative type I PSC volume (Fig. 6a); the PSC volume V_{nat} expressed in percent of the air volume in the hemispherical layer between the isentropic surfaces 390 and 580 K (Fig. 6b), and the polar vortex volume V_{vort} expressed in the same units (Fig. 6c). The absolute values of the type I PSC volume and the stratospheric polar vortex volume were also calculated for each of the HIST1-5 experiments.

The maximal relative type I PSC volume reaches 0.20, which is a little less than the value in data of four reanalyses (0.3–0.35). The comparison with the reanalysis data [36] shows that the polar vortex occupies a much larger volume (by ~1.5 times) in the INM RAS model than in the ERA-Interim and MERRA data. At the same time, the absolute PSC volume in model calculations is comparable with the reanalysis data.

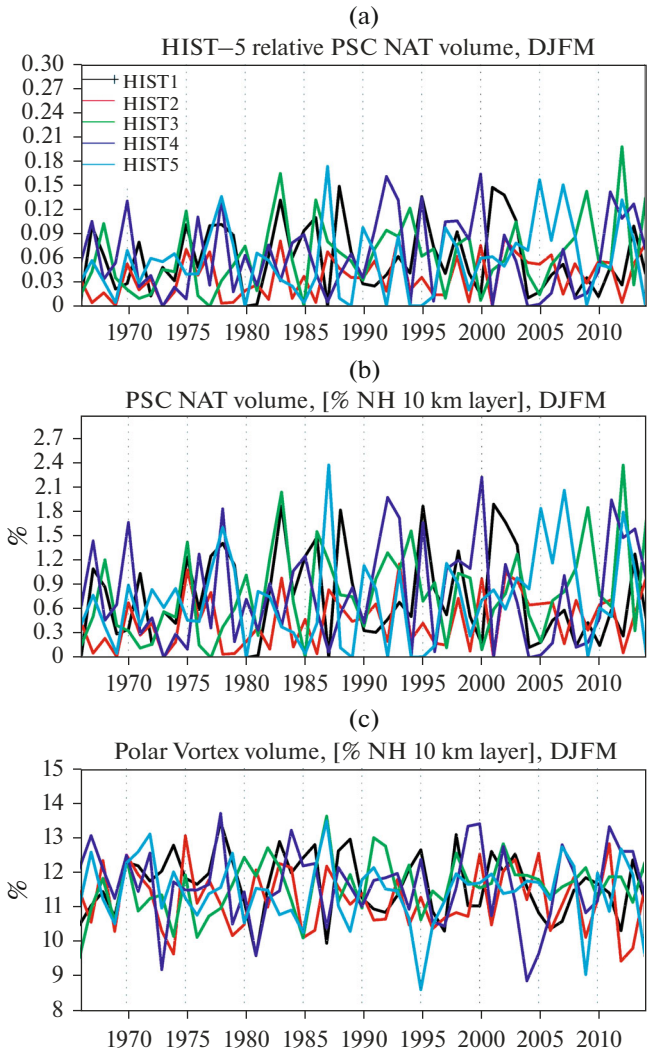

Fig. 6. Arctic stratospheric polar-vortex parameters over a 50-year period of HIST1–5 model calculations when averaging over December–March: (a) ratio of PSC volume to the stratospheric polar vortex volume V_{nat}/V_{vort}; (b) PSC volume V_{nat} expressed in percent of the air volume in the hemispherical layer between the isentropic surfaces of 390 and 580 K; (c) polar vortex volume V_{vort} expressed in percent of the air volume in the hemispherical layer between isentropic surfaces of 390 and 580 K.

The maximal winter average (December–March) values of the absolute PSC volume calculated in the model and found from the MERRA-2 reanalysis were compared. The highest values in the reanalysis data are ~52 million km^3 in winter 2011, with the maximal ozone layer depletion in the Arctic [6]. Some winter seasons can be distinguished in the model calculations, with comparable values of the maximal PSC volumes from 50 to 60 million km^3, for example, ~60 million km^3 in 2012 (HIST3) and 1987 (HIST5); ~56 million km^3 in 2000 (HIST4); and ~50 million km^3 in 1983 (HIST3), 1992 (HIST4), and 2007 (HIST5).

3.3. Correlation between Spring Breakup Dates and PSC Parameters

Since spring breakup events complete the period of existence of the stratospheric polar vortex, one can assume that winter seasons with late spring breakup events should be characterized by a large PSC volume. However, the results show a weak but negative correlation in the MERRA-2 reanalysis data and the model calculations (Fig. 7). A statistically significant (95% by the Student's test) correlation has been revealed in the reanalysis data and the HIST3 data (Table 1). A similar weak negative correlation has been revealed when using the relative (normalized to the stratospheric polar vortex volume) and integral (daily total) values of the PSC volume.

The small negative correlation between the spring breakup dates and the PSC volume can be explained as follows. The PSC volume is usually maximal in end of January to first half of February at altitudes of 30–70 hPa; therefore, the winter average PSC volume to a large extent characterizes the temperature just in this time interval and at these altitudes. A spring breakup event occurs on average in March–April and is detected by the wind speed at 10 hPa. Positive temperature anomalies in the Arctic stratosphere at this time and at this altitude usually mean an earlier spring breakup date. According to the results [37], the 1st empirical orthogonal function (EOF) of intraseasonal temperature variability in the Arctic stratosphere behaving as an anomaly at 30–70 hPa at the end of January and first half of February is followed by an anomaly of the opposite sign at 10 hPa in March–April (see Fig. 1). Thus, the negative correlation between the PSC volume and the spring breakup date is due to the fact that a negative temperature anomaly at 30–70 hPa in the end of January and first half of February is usually followed by a positive temperature anomaly at 10 hPa in March–April. In other words, after a period of low temperatures in the Arctic lower stratosphere in January and the first half of February, when a large PSC volume is formed, a significant warming occurs in the middle stratosphere with a spring breakup event in March–April.

The underestimated negative correlation in the model calculations in comparison with the reanalysis data can be partly explained by the fact that the INM RAS model version under study has no interactive chemistry block and, hence, there is no feedback between the ozone layer depletion and a decrease in the temperature of the lower stratosphere and strengthening of the stratospheric polar vortex.

4. CONCLUSIONS

The study of spring breakup events, PSC volume, and their interannual variability in five 50-year calculations in the INM RAS climate model version 5 in

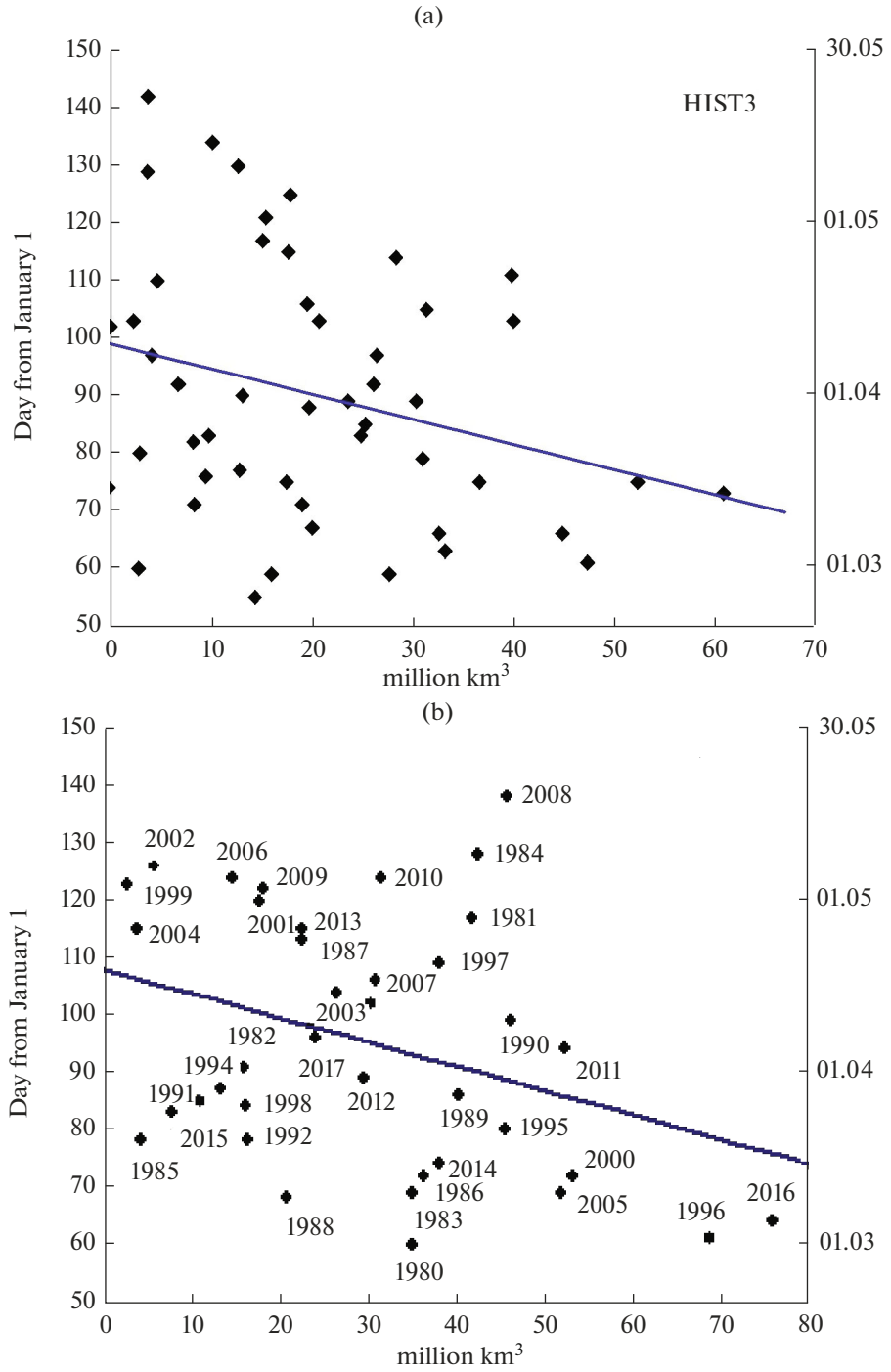

Fig. 7. Scatter diagrams of spring breakup dates in the Arctic and the winter averaged (December–March) absolute PSC volumes (million km^3) according to (a) HIST3 model calculation and (b) MERRA-2 and ERA-Interim data.

comparison with the reanalysis data allows us to draw the following conclusions.

—The spring breakup dates in model calculations vary within a two-months range, from March to May, which is consistent with the estimates based on the reanalysis data.

—The climatological date of the spring breakup event is April 4 according to the ERA-Interim reanalysis data; in model calculations, it varies from March 27 to April 1, which is consistent with the results [18], where this date is March 30 according to the NCEP reanalysis data.

—An insignificant trend in the shift of spring breakup events at later dates was revealed in the ERA-Interim data for 1980–2017. Among all model experiments, only HIST2 shows a positive trend of interan-

nual variability of the breakup event date over 49 years, but this trend is insignificant.

—The significant linear correlation revealed between the spring breakup dates and SPW1 amplitude in March (correlation coefficient is 0.62) shows that early breakup events are accompanied by strong wave activity, and the wave activity is weaker during late breakup events and they are caused by seasonal heating of the middle atmosphere. The results of model experiments show a negative linear correlation between the spring breakup dates and SPW1 amplitude in March; significant coefficients have been obtained for the HIST1–3 experiments.

—REM temperature minimum required for type I PSC formation occurs earlier, from mid or early December, and at higher altitudes, near 20–30 hPa, than in the INM RAS model calculations (early January and 30–40 hPa). The maximal PSC area approximately corresponds to the REM value. However, as in the case of extreme temperatures, PSCs in the INM RAS model data appear half a month to a month later and disappear at approximately the same time as REM (early-to-mid March). In the model calculations, the stratospheric polar vortex occupies a ~1.5-time larger volume than in the ERA-Interim and MERRA data.

(i) The maximal relative PSC volume in the model calculations reaches ~0.20, which is slightly less than in the data of four reanalyses (0.3–0.35). At the same time, the model calculations revealed winter seasons with the maximal absolute PSC volume (50–60 million km^3), comparable to the values calculated from the MERRA-2 reanalysis data for winter 2011 with the record ozone layer depletion in the Arctic.

(ii) After a period of low temperatures in the Arctic lower stratosphere in January and the first half of February, which results in the formation of a large PSC volume, a significant warming occurs in the middle stratosphere in March–April on average, accompanied by an early spring breakup event.

FUNDING

This work was financially supported by the Russian Foundation for Basic Research (project no. 19-05-00370). The study of the effect of global processes on the Arctic stratosphere was partially supported by the Russian Science Foundation (grant no. 19-17-00198).

REFERENCES

1. N. Pedatella, J. Chau, H. Schmidt, L. Goncharenko, C. Stolle, K. Hocke, V. Harvey, B. Funke, and T. Siddiqui, "How sudden stratospheric warming affects the whole atmosphere," Trans., Am. Geophys. Union **99** (2018).
2. M. Baldwin and T. Dunkerton, "Stratospheric harbingers of anomalous weather regimes," Science **294,** 581–584 (2001).
3. E. Kolstad, T. Breiteig, and A. Scaife, "The association between stratospheric weak polar vortex events and cold air outbreaks in the Northern Hemisphere," Q. J. R. Meteorol. Soc **136,** 886–893 (2010).
4. L. Tomassini, E. Gerber, M. Baldwin, F. Bunzel, and M. Giorgetta, "The role of stratosphere-Troposphere coupling in the occurrence of extreme winter cold spells over Northern Europe," J. Adv. Modeling Earth Syst. **4,** A03 (2012).
5. D. Nath, W. Chen, C. Zelin, A. Pogoreltsev, and K. Wei, "Dynamics of 2013 sudden stratospheric warming event and its impact on cold weather over Eurasia: Role of planetary wave reflection," Sci. Rep. **6,** 24174 (2016).
6. G. Manney, M. Santee, M. Rex, N. Livesey, M. Pitts, P. Veefkind, E. Nash, I. Wohltmann, R. Lehmann, L. Froidevaux, L. Poole, M. Schoeberl, D. Haffner, J. Davies, V. Dorokhov, H. Gernandt, B. Johnson, R. Kivi, E. Kyro, N. Larsen, P. Levelt, A. Makshtas, C. McElroy, H. Nakajima, M. Parrondo, D. Tarasick, P. Gathen, K. Walker, and N. Zinoviev, "Unprecedented Arctic ozone loss in 2011," Nature **478,** 469–475 (2011).
7. U. Langematz, S. Meul, K. Grunow, E. Romanowsky, S. Oberlander, J. Abalichin, and A. Kubin, "Future Arctic temperature and ozone: The role of stratospheric composition changes," J. Geophys. Res. **119,** 2092–2112 (2014).
8. A. Karpechko, L. Backman, L. Tholix, I. Ialongo, M. Andersson, V. Fioletov, A. Heikkila, B. Johnsen, T. Koskela, E. Kyrola, K. Lakkala, C. Myhre, M. Rex, V. Sofieva, J. Tamminen, and I. Wohltmann, "The link between springtime total ozone and summer UV radiation in Northern Hemisphere extratropics," J. Geophys. Res. **118,** 8649–8661 (2013).
9. F. Khosrawi, O. Kirner, B-M. Sinnhuber, S. Johansson, M. Hopfner, M. Santee, L. Froidevaux, J. Ungermann, R. Ruhnke, W. Woiwode, H. Oelhaf, and P. Braesicke, "Denitrification, dehydration and ozone loss during the 2015/2016 Arctic winter," Atmos. Chem. Phys. **17,** 12893–12910 (2017).
10. N. Calvo, L. Polvani, and S. Solomon, "On the surface impact of Arctic stratospheric ozone extremes," Environ. Res. Lett **10,** 094003 (2015).
11. P. N. Vargin, M. P. Nikiforova, and A. M. Zvyagintsev, "Variability of the Antarctic ozone anomaly in 2011–2018," Russ. Meteorol. Hydrol. **45,** 63–73 (2020).
12. R. X. Black and B. A. McDaniel, "The dynamics of Northern Hemisphere stratospheric final warming events," J. Atmos. Sci. **64,** 2932–2946 (2007).
13. D. W. Waugh, W. J. Randel, S. Pawson, P. A. Newman, and E. R. Nash, "Persistence of the lower stratospheric polar vortices," J. Geophys. Res. **104,** 27191–27201 (1999).
14. M. Salby and P. Callaghan, "Influence of planetary wave activity on the stratospheric final warming and spring ozone," J. Geophys. Res. **112,** D20111 (2007).
15. D. Cayan, S. Kammerdiener, M. Dettinger, J. Caprio, and D. Peterson, "Changes in the onset of spring in the Western United States," Bull. Am. Meteorol. Soc. **82** (3), 399–415 (2001).

16. B. Ayarzagüena and E. Serrano, "Monthly characterization of the tropospheric Circulation over the Euro-Atlantic area in relation with the timing of stratospheric Final warming," J. Clim. **22,** 6313–6324 (2009).
17. S. Hardiman, N. Butchart, A. Charlton-Perez, T. Shaw, H. Akiyoshi, A. Baumgaertner, S. Bekki, P. Braesicke, M. Chipperfield, M. Dameris, R. Garcia, M. Michou, S. Pawson, E. Rozanov, and K. Shibata, "Improved predictability of the troposphere using stratospheric final warmings," J. Geophys. Res. **116,** D18113 (2011).
18. E. N. Savenkova, A. Yu. Kanukhina, A. I. Pogoreltsev, and E. G. Merzlyakov, "Variability of the springtime transition date and planetary waves in the stratosphere," J. Atmos. Sol.-Terr. Phys. **90-91,** 1–8 (2012).
19. R. Thieblemont, B. Ayarzagüena, K. Matthes, S. Bekki, J. Abalichin, and U. Langematz, "Drivers and surface signal of inter-annual variability of boreal stratospheric final warmings," J. Geophys. Res. **124** (11), 5400–5417 (2019).
20. G. Manney, N. Livesey, C. Jimenez, H. Pumphrey, M. Santee, I. MacKenzie, and J. Waters, "EOS microwave limb sounder observations of "frozen-in" anticyclonic air in Arctic summer," Geophys. Res. Lett. **33,** L06810 (2006).
21. R. Thieblemont, Y. Orsolini, A. Hauchecorne, M.-A. Drouin, and N. Huret, "A climatology of frozen-in anticyclones in the spring Arctic stratosphere over the period 1960–2011," J. Geophys. Res. **118,** 1299–1311 (2013).
22. A. Butler, A. Charlton-Perez, D. Domeisen, I. Simpson, and J. Sjoberg, "Predictability of Northern Hemisphere final stratospheric warmings and their surface impacts," Geophys. Res. Lett. **46** (17–18), 10578–10588 (2019).
23. *Ozone. WMO Report No.55. Scientific Assessment of Ozone Depletion. 2018* (WMO, 2018).
24. M. Rex, R. Salawitch, P. Gathen, N. Harris, M. Chipperfield, and B. Naujokat, "Arctic ozone loss and climate change," Geophys. Res. Lett. **31,** L04116 (2004).
25. S. P. Smyshlyaev, A. I. Pogorel'tsev, V. Ya. Galin, and E. A. Drobashevskaya, "Influence of wave activity on the composition of the polar stratosphere," Geomagn. Aeron. **56** (1), 102–116 (2016).
26. E. M. Volodin, E. V. Mortikov, S. V. Kostrykin, V. Ya. Galin, V. N. Lykosov, A. S. Gritsun, N. A. Diansky, A. V. Gusev, and N. G. Yakovlev, "Simulation of modern climate with the new version of the INM RAS climate model," Izv., Atmos. Oceanic Phys. **53,** 142–155 (2017).
27. E. M. Volodin and S. V. Kostrykin, "The aerosol module in the INM RAS climate model," Russ. Meteorol. Hydrol. **41** (8), 519–528 (2016).
28. P. N. Vargin and E. M. Volodin, "Analysis of the reproduction of dynamic processes in the stratosphere using the climate model of the Institute of Numerical Mathematics, Russian Academy of Sciences," Izv., Atmos. Oceanic Phys. **52,** 1–15 (2016).
29. P. N. Vargin, S. V. Kostrykin, and E. M. Volodin, "Analysis of simulation of stratosphere-troposphere dynamical coupling with the INM-CM5 climate model," Russ. Meteorol. Hydrol. **43,** 780–786 (2018).
30. B. Ayarzagüena, A. Charlton-Perez, A. Butler, P. Hitchcock, I. Simpson, L. Polvani, N. Butchart, E. Gerber, L. Gray, B. Hassler, P. Lin, F. Lott, E. Manzini, R. Mizuta, C. Orbe, S. Osprey, D. Saint-Martin, M. Sigmond, M. Taguchi, E. Volodin, and S. Watanabe, "Uncertainty in the response of sudden stratospheric warmings and stratosphere-troposphere coupling to quadrupled CO_2 concentrations in CMIP6 models," J. Geophys. Res.: Atmos. **125** (6), e2019-JD032345 (2020).
31. Z. Lawrence, G. Manney, and K. Wargan, "Reanalysis intercomparisons of stratospheric polar processing diagnostics," Atmos. Chem. Phys. **18,** 13547–13579 (2018).
32. K. Wei, W. Chen, and R. Huang, "Dynamical diagnosis of the breakup of the stratospheric polar vortex in the Northern Hemisphere," Sci. China, Ser. D: Earth Sci. **50** (9), 1369–1379 (2007).
33. A. A. Pogoreltsev, E. Savenkova, O. Aniskina, T. Ermakova, W. Chen, and K. Wei, "Interannual and intraseasonal variability of stratospheric dynamics and stratosphere–troposphere coupling during Northern winter," J. Atmos. Sol.-Terr. Phys., **136,** 187–200 (2015).
34. E. V. Rakushina, T. S. Ermakova, and A. I. Pogoreltsev, "Changes in the zonal mean flow, temperature, and planetary waves observed in the Northern Hemisphere mid-winter months during the last decades," J. Atmos. Sol.-Terr. Phys **171,** 234–240 (2018).
35. K. K. Kandieva, O. G. Aniskina, A. I. Pogoreltsev, O. S. Zorkaltseva, and V. I. Mordvinov, "Effect of the Madden–Julian oscillation and quasi-biennial oscillation on the dynamics of extratropical stratosphere," Geomagn. Aeron. **59** (1), 105–114 (2019).
36. Z. Lawrence, G. Manney, K. Minschwaner, M. Santee, and A. Lambert, "Comparisons of polar processing diagnostics from 34 years of the ERA-Interim and MERRA reanalyses," Atmos. Chem. Phys. **15,** 3873–3892 (2015).
37. V. V. Vorobyeva and E. M. Volodin, "Investigation of the structure and predictability of the first mode of stratospheric variability based on the INM RAS climate Model," Russ. Meteorol. Hydrol. **43,** 737–742 (2018).

Translated by O. Ponomareva